Received July 3, 2019, accepted July 30, 2019, date of publication August 2, 2019, date of current version August 26, 2019.

Digital Object Identifier 10.1109/ACCESS.2019.2932955

Joint Multiple Relay Selection and Time Slot Allocation Algorithm for the EH-Abled Cognitive Multi-User Relay Networks

HONGYUAN GAO[1], (Member, IEEE), SHIBO ZHANG[1], YUMENG SU[1], MING DIAO[1], AND MINHO JO[2], (Senior Member, IEEE)

[1]College of Information and Communication Engineering, Harbin Engineering University, Harbin 150001, China
[2]Department of Computer and Information Science, Korea University, Sejong City 30019, South Korea

Corresponding author: Minho Jo (minhojo@korea.ac.kr)

This work was supported in part by the National Research Foundation of the Korean Government under Grant NRF-2016R1D1A1B03932149, in part by the National Natural Science Foundation of China under Grant 61571149, in part by the Fundamental Research Funds for the Central Universities under Grant HEUCFP201808, in part by the Special China Postdoctoral Science Foundation under Grant 2015T80325, in part by the Fundamental Research Funds for the Central Universities under Grant HEUCF190801, and in part by the China Postdoctoral Science Foundation under Grant 2013M530148.

ABSTRACT The wireless energy harvesting (EH) technique is regarded as a new way to provide an energy supply for energy-constrained cognitive relay networks (CRNs). A novel wireless EH cognitive multi-user relay network (CMRN) for the underlay protocol is investigated in this paper. In this system, there are multiple primary users (PUs) and multiple secondary users (SUs). The SUs can share the licensed spectrum and harvest energy from ambient signals. The problems of multiple relay selection by the SUs and of finding the optimal EH ratio are considered. We analytically derive the exact expression of the throughput of a secondary network. In it, there are four constraints: for the permitted peak interference with each primary transmitter (PT); for the sum interference for each PT; that the transmit power of secondary source nodes (SSNs) and secondary relays (SRs) should be less than the energy harvested; and that each secondary source node/secondary destination node (SSN-SDN) pair can only choose one SR. To obtain the optimal performance of the secondary network's throughput, we should optimize the multiple relay selection scheme and the EH ratio. Actually, it is a classic integer optimization problem to design an optimal multiple relay selection scheme. However, the selection of the optimal EH ratio is a continuous optimization problem. The joint multiple relay selection and time slot allocation is a classical hybrid optimization problem. So, we propose a novel quantum sine cosine algorithm (QSCA) for resolving the difficulty with optimization of multiple relay selection and the EH ratio. Our simulation results verify our proposed solution by showing the influence of different parameters for the proposed model and by demonstrating good performance under the QSCA.

INDEX TERMS Cognitive relay networks, wireless energy harvesting, multiple primary users, multiple secondary users, multiple relay selection.

I. INTRODUCTION

With the increasing demand for wireless transmission and green communications, the efficiency of both spectrum and energy has been an essential concern for wireless communications [1]–[3]. Due to the fact that the technologies of cognitive radio and cooperative communications are able to make cognitive relay networks (CRNs) more reliable in their application, the recent work mainly pays attention to cooperative communications in cognitive networks [4]–[6]. In this case, various CRNs are proposed to address the lack of spectrum [7]–[9]. For a cognitive network, the secondary users (SUs) are able to use the licensed spectrum of the primary users (PUs). An underlay protocol was proposed [10]–[13] in which the SU is able to share the same spectrum of the PU when it transmits its own signal, and SU does not have too much interference on the transmission of the PU. In [10], Guo *et al*. investigated cooperative

The associate editor coordinating the review of this article and approving it for publication was Giuseppe Araniti.

communications between two secondary users with the underlay protocol, and then, they derived the outage probability of the system model. In a study by Duong *et al*. [12], there are multiple PUs in the system model. The underlay protocol was studied further, and the influence of different parameters was verified by the simulation results.

Energy harvesting (EH) technology is applied to cases where energy is limited in order to provide extra energy for information transmission, decoding, and some other communication work [14], [15]. To take advantage of EH, many studies have been undertaken in recent years [16]–[19]. Recently, fixed energy storage for EH was considered [16], [20]. The authors considered the energy allocation problem with time-varying channel conditions and energy resources, and solved it with a water-filling energy allocation solution. In [19], for a secrecy cooperative network, the relay nodes were able to collect energy from ambient signals. The authors discussed the outage probability, and then gave mathematical formulas for it.

To take advantage of wireless EH and CRNs, recent work focused on combining them [21]–[23]. The combination of EH and CRN technology has become a hot topic in recent years. In [24], the SU was able to collect energy from the PU and then store it in the battery of the secondary user. The authors studied the optimal sensing time of the system model and maximized the harvested energy. In [25], the authors proposed a new protocol for EH and information transmission in CRNs. The authors investigated three sets of circumstances for the system, making it into a biconvex problem to be solved. In [26], a wireless EH method was applied to CRNs. To analyze the performance of the system model, an accurate outage probability and the closed-form outage probability were derived when the number of PU transceivers reached infinity.

Relay selection is an important technology in modern telecommunications [27]–[29]. In the past, there were articles about simple user-relay selections, but there has been little study about multi-user and multi-relay networks. For the multi-user and multi-relay network, each user aims to find a suitable relay in order to get optimal performance for information transmission [30]. In [31], an algorithm was designed for maximizing the transmission rate in a multi-user and multi-relay network. In [32] and [33], the authors presented novel relay selection methods to maximize the minimum achievable transmission rate. But some authors did not consider co-channel interference (CCI) in the network [31]–[33]. To solve this problem, Singh *et al*. [34] considered CCI among multiple users, and then suggested a relay selection scheme. However, only a sub-optimal solution was obtained.

While previous studies have made significant progress in designing a better system for a CRN and EH, there are still some aspects to improve. First of all, existing EH CRN systems [22]–[25] mostly considered the situation where there are multiple SUs or multiple PUs. The researches on joint multiple relay selection and time slot allocation problem for CRN communications where there are multiple SUs and multiple PUs are very few. However, due to the growth of number of users and the increase of network throughput requirements, the future reality is more of a multi-user scenario in communications networks. Hence, it is imperative to investigate the joint multiple relay selection and time slot allocation problem for the EH CRNs. Second, previous multiple relay selection research [31]–[34] only gave a simple multiple relay selection strategy or relay allocation approach without considering CCI or the optimal solution due to the difficulty of multiple constraints and the complexity of computations. It is necessary to investigate an optimal multiple relay selection scheme for multiple SUs in an underlay network. Furthermore, existing works, such as that by Liu *et al*. [26], only considered a fixed time slot structure model, and could not obtain optimal EH CRN system parameters for improving the performance of the communications system.

To maximize the utilization of energy transmission, an interesting method of using unlicensed bands for additional transmissions of the licensed band was proposed [35]. The proposed method uses both licensed bands and unlicensed bands, which is different from traditional wireless energy harvesting, but they did not consider CRNs.

In order to overcome the limitations in the existing methods and to obtain a more extensive application for the actual scenarios, it is necessary to design a novel wireless EH CMRN system model where there are multiple PUs and multiple SUs. For the model investigated in this paper, the SUs share the same licensed spectrum with the PUs. There are multiple relays for the secondary users to select for transmitting their own information. Each SU selects a suitable relay. For the secondary network, each secondary source node (SSN) and each secondary relay (SR) can collect energy from ambient signals. The SUs make use of the energy harvested to transmit their own information. However, for the secondary network, transmission quality is impacted by the PUs because of some interference constraints. In addition, the joint multiple relay selection and time slot allocation scheme also affects the performance of the secondary network. To maximize throughput in the secondary network, we propose a novel quantum sine cosine algorithm (QSCA) to obtain the optimal time slot allocation and multiple relay selection scheme under various network constraints. The contributions in this paper are summarized in the following.

- We investigate a CMRN with wireless EH for a cognitive system under the circumstances of multiple PUs and multiple SUs. In this model, the SUs are able to collect energy from ambient signals and then finish their own transmissions. Each secondary user selects the best relay for its transmission. In addition, the structure of the time slot is also studied.
- We derive analytical formulas for the throughput of the proposed new model. The analytical expression has proven that an optimal multiple relay selection scheme and EH ratio can maximize the throughput of the secondary network. Besides, the throughput of the CMRN

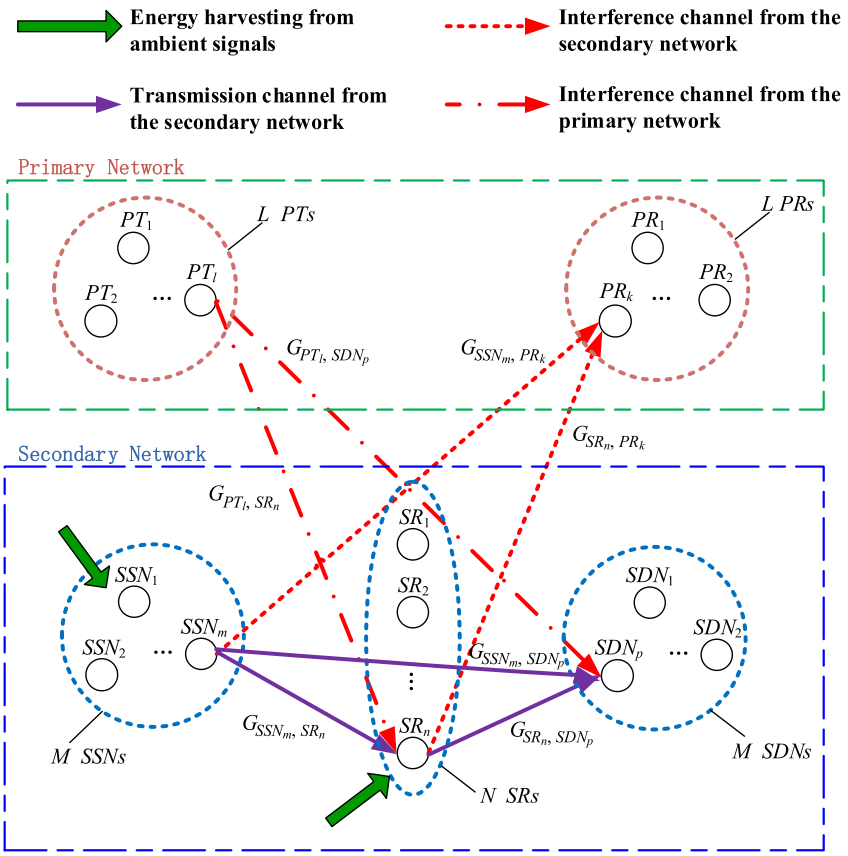

FIGURE 1. System model of the proposed CMRN with wireless EH.

is subject to four constraints: 1) on the permitted peak interference of each primary transmitter (PT) influenced by SSNs and SRs, 2) on the sum interference of each primary transmitter influenced by SSNs and SRs, 3) on the maximum transmit power of SSNs and SRs, and 4) that each secondary source node/secondary destination node (SSN-SDN) pair only can choose one SR.

- We propose a QSCA to find the optimal multiple relay selection scheme and EH ratio. The multiple relay selection is an integer problem, but the EH ratio problem is a continuous problem. Many traditional continuous intelligent algorithms cannot be directly applied to resolving this problem. So, we put forward a novel algorithm—QSCA—to solve it. The simulations indicate that the QSCA proposed has better performance under different circumstances, compared to other evolution strategies. We have also investigated the throughput of the proposed wireless EH CMRN based on various system parameters, e.g., the number of secondary transmission pairs, the number of SRs, the EH rate of the SSNs, the EH rate of the SRs, and the interference threshold of primary receivers (PRs).

The rest of this paper is organized as follows. In Section II, we propose the system model, and then, we show the EH and information transmission time-slot structure. In Section III, we derive the analytical expression of the secondary network's throughput. For Section IV, the novel QSCA is proposed for finding the optimal multiple relay selection scheme and EH ratio in order to maximize the throughput of the secondary network. The simulation results and conclusion are provided in sections V and VI, respectively.

II. SYSTEM MODEL

A. STRUCTURE OF CMRN

In this paper, an underlay CMRN with wireless EH is considered. As shown in Fig. 1, the primary network consists of L PTs and L PRs. Each PT has its own information to transmit to a PR. Then, the primary network formulates L PT–PR transmission pairs. The secondary network is made up of M SSNs, M secondary destination nodes (SDNs), and N SRs. The secondary network consists of M SSN-SDN transmission pairs. For a cooperative multi-user and multi-relay secondary network, N is usually larger than M [30], [36]. Each SSN-SDN transmission pair selects one SR to complete a transmission, and the SR recodes information and then sends the information to its corresponding SDN. In the secondary network, SSNs and SRs collect energy from ambient signals, whereas SDNs do not collect energy. All the energy collected by SSNs and SRs is used to transmit information. All the SSNs and SRs have the ability to store the harvested energy. In this model, the energy storage unit can be a super capacitor, and the harvested energy should be used in one time slot.

Since SUs can share the spectrum of the PUs, the transmission of PT-PR pairs is impacted by the secondary network [11]. Interference with the PRs by the SUs should be considered, and the interference should remain below a certain threshold. We represent the threshold as I_{th}. Also, the PTs will impact the SSNs and SRs [26]. The main notations of CMRN with EH are shown in the TABLE 1.

TABLE 1. Main notations of CMRN with EH.

Notation	Description
G_{SSN_m,PR_k}	CSI from the mth SSN to the kth PR
G_{SR_n,PR_k}	CSI from the nth SR to the kth PR
G_{PT_l,SR_n}	CSI from the lth PT to the nth SR
G_{PT_l,SDN_p}	CSI from the lth PT to the pth SDN
G_{SSN_m,SR_n}	CSI from the mth SSN to the nth SR
G_{SR_n,SDN_p}	CSI from the nth SR to the pth SDN
α	EH ratio
T	Time slot duration
Y_{SSN_m}	EH rate of the mth SSN
Y_{SR_n}	EH rate of the nth SR
E_{SSN_m}	Energy stored for the mth SSN
E_{SR_n}	Energy stored at the nth SR
I_{th}	Interference threshold of PU
P_{SR_n}	Transmit power for the nth SR
P_{PT_l}	Transmit power of the lth PT
$\gamma_m^{SSN,SDN}$	SINR of the mth SSN-SDN link
$\gamma_m^{SSN,SR}$	SINR of the mth SSN-SR link
$\gamma_m^{SR,SDN}$	SINR of the mth SR-SDN link
γ_m	End-to-end SINR of the mth SSN-SDN pair
R_m	Throughput of the mth secondary user
R^{total}	Throughput of the secondary network

For the CMRN, each transmission channel is a Rayleigh fading channel. For the same time slot, the channel state information (CSI) between two nodes is the same. However, for two different time slots, the CSI from one is independent of the others. The CSI from the mth ($m = 1, 2, \ldots, M$) SSN to the kth($k = 1, 2, \ldots, L$) PR is denoted as G_{SSN_m,PR_k}, the CSI from the nth ($n = 1, 2, \ldots, N$) SR to the kth PR is denoted as G_{SR_n,PR_k}, the CSI from the lth($l = 1, 2, \ldots, L$) PT to the nth SR is denoted as G_{PT_l,SR_n}, the CSI from the lth PT to the pth($p = 1, 2, \ldots, L$) SDN is denoted as G_{PT_l,SDN_p}, the CSI from the mth SSN to the nth SR is denoted as G_{SSN_m,SR_n}, the CSI from the mth SSN to the pth SDN is denoted as G_{SSN_m,SDN_p}, and the CSI from the nth SR to the pth SDN is denoted as G_{SR_n,SDN_p}.

We represent the distance between the mth SSN and the kth PR as d_{SSN_m,PR_k}, and the distance between the nth SR and the kth PR is represented as d_{SR_n,PR_k}. Similarly, the distance between the lth PT and the nth SR, the distance between the lth PT and the pth SDN, the distance between the mth SSN and the nth SR, the distance between the mth SSN and the pth SDN, and the distance between the nth SR and the pth SDN are represented as d_{PT_l,SR_n}, d_{PT_l,SDN_p}, d_{SSN_m,SR_n}, d_{SSN_m,SDN_p} and d_{SR_n,SDN_p}, respectively. CSI G_{SSN_m,PR_k}, G_{SR_n,PR_k}, G_{PT_l,SR_n}, G_{PT_l,SDN_p}, G_{SSN_m,SR_n}, G_{SSN_m,SDN_p}, and G_{SR_n,SDN_p} follow an exponential distribution with parameters $d_{SSN_m,PR_k}^{-\beta}$, $d_{SR_n,PR_k}^{-\beta}$, $d_{PT_l,SR_n}^{-\beta}$, $d_{PT_l,SDN_p}^{-\beta}$, $d_{SSN_m,SR_n}^{-\beta}$, $d_{SSN_m,SDN_p}^{-\beta}$, and $d_{SR_n,SDN_p}^{-\beta}$, respectively, in which β is the path loss factor. They are individually, independently, and statistically distributed.

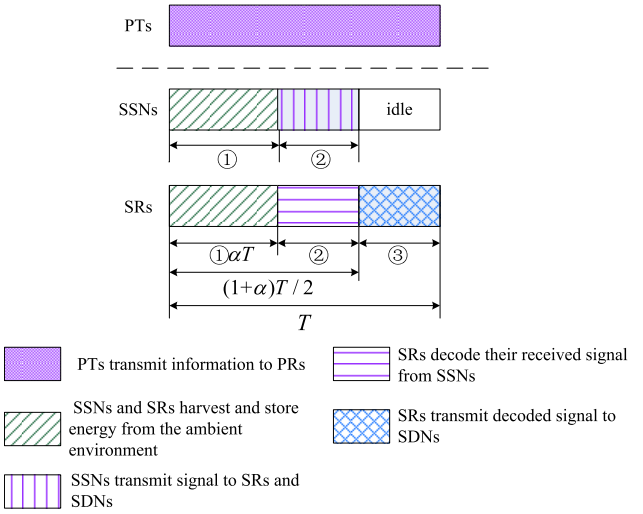

FIGURE 2. Structure of the time slot.

B. STRUCTURE OF THE TIME SLOT

Fig. 2 shows the activities of EH and information transmission for one time slot of the CMRN. Each PT transmits information to its corresponding PR all the time. Meanwhile, the secondary network transmits its own information. A time slot of the secondary network is composed of three parts, as follows.

① SSNs and SRs collect energy from the surrounding signals, and then store it for information transmission, and α is the EH ratio, $0 \leq \alpha \leq 1$. EH ratio is the time ratio for harvested energy in one time slot, and T is the duration of one time slot.

② SSNs transmit signals to SRs and SDNs. In SRs, SRs decode the received signal.

③ SRs transmit the decoded signals to SDNs, and SDNs incorporate the signal from SSNs and SRs via maximum ratio combining (MRC) [23].

III. THROUGHPUT ANALYSIS OF THE SECONDARY NETWORK

EH and the information transmission protocol include three time phases. Each PT transmits information to its corresponding PR all the time. The secondary network works in different modes in different time slots. We will here derive an analytical expression for the throughput of the secondary network.

A. EH OF THE SECONDARY NETWORK (PHASE 1)

In Phase 1, SSNs and SRs collect energy from ambient signals. The energy stored for the mth SSN is calculated as

$$E_{SSN_m} = \alpha Y_{SSN_m} T, \tag{1}$$

where Y_{SSN_m} is the EH rate of the mth SSN and EH rate represents the amount of energy harvested in unit time [8], [37], [38].

The energy stored in the nth SR is calculated as

$$E_{SR_n} = \alpha Y_{SR_n} T, \tag{2}$$

where Y_{SR_n} is the EH rate of the nth SR. We assume that SSNs and SRs use constant power to transmit signals during a time slot, so the maximum transmit power provided by SSNs and SRs will be

$$P_{SSN_m}^{\max} = \frac{E_{SSN_m}}{(1-\alpha)T/2}, \tag{3}$$

and

$$P_{SR_n}^{\max} = \frac{E_{SR_n}}{(1-\alpha)T/2}, \tag{4}$$

respectively.

The secondary network should satisfy the power constraint of the PUs [10]; that is to say, the interference with PRs produced by SSNs and SRs, respectively, should remain below a certain threshold, I_{th}, which are calculated as

$$\sum_{m=1}^{M} P_{SSN_m} G_{SSN_m,PR_k} \le I_{\text{th}}, \tag{5}$$

and

$$\sum_{n=1}^{N} P_{SR_n} G_{SR_n,PR_k} \le I_{\text{th}}. \tag{6}$$

In order to satisfy these constraints, the power of each SSN and SR should be limited to two defined values, $P_{SSN_m}^{\lim}$ and $P_{SR_n}^{\lim}$, which are inversely proportional to CSI G_{SSN_m,PR_k} and G_{SR_n,PR_k}, respectively:

$$P_{SSN_m}^{\lim} = \frac{I_{\text{th}}}{M(\max(G_{SSN_m,PR_k}))}, \tag{7}$$

and

$$P_{SR_n}^{\lim} = \frac{I_{\text{th}}}{M(\max(G_{SR_n,PR_k}))}, \tag{8}$$

where $\max(\cdot)$ is the function for taking the maximum value of the matrix.

Considering the factor of the power limitation [11], the transmit power for the mth SSN and the nth SR, respectively, can be represented as follows:

$$\begin{aligned} P_{SSN_m} &= \min(P_{SSN_m}^{\max}, P_{SSN_m}^{\lim}) \\ &= \min\left(\frac{E_{SSN_m}}{(1-\alpha)T/2}, \frac{I_{\text{th}}}{M(\max(G_{SSN_m,PR_k}))}\right), \end{aligned} \tag{9}$$

and

$$\begin{aligned} P_{SR_n} &= \min(P_{SR_n}^{\max}, P_{SR_n}^{\lim}) \\ &= \min\left(\frac{E_{SR_n}}{(1-\alpha)T/2}, \frac{I_{\text{th}}}{M(\max(G_{SR_n,PR_k}))}\right). \end{aligned} \tag{10}$$

B. INFORMATION TRANSMISSION (PHASES 2 AND 3)

For Phase 2 of the time slot, SSNs transmit signals to SDNs and SRs. During this time interval, one SSN can only select one SR to relay information. There is only one available channel for one SSN-SDN transmission pair. A decode-and-forward (DF) transmission mode is applied in the system. The mth SSN sends z_m, where z_m is the information symbol. If z_m can be normalized by $E|z_m|^2 = 1$, the average power of the mth SSN is denoted by P_{SSN_m}. The lth PT sends x_l to lth PR, where x_l is the information symbol. The transmit power of the lth PT is P_{PT_l}.

For the mth SDN, the received signal at the mth SDN is

$$\begin{aligned} y_m^{SSN,SDN} &= \sqrt{G_{SSN_m,SDN_m}}\sqrt{P_{SSN_m}} z_m \\ &\quad + \sum_{j=1,j\neq m}^{M} \sqrt{G_{SSN_j,SDN_m}}\sqrt{P_{SSN_j}} z_j \\ &\quad + \sum_{l=1}^{L} \sqrt{G_{PT_l,SDN_m}}\sqrt{P_{PT_l}} x_l + w_1, \end{aligned} \tag{11}$$

where w_1 represents additive white Gaussian noise (AWGN); η_1 is power, with $\sum_{j=1,j\neq m}^{M} \sqrt{G_{SSN_j,SDN_m}}\sqrt{P_{SSN_j}} z_j$ and $\sum_{l=1}^{L} \sqrt{G_{PT_l,SDN_m}}\sqrt{P_{PT_l}} x_l$ as the interference signals created by the other SSNs and PTs at the mth SDN, so the signal-to-interference-plus-noise ratio (SINR) of the SSN-SDN link is derived as follows:

$$\gamma_m^{SSN,SDN} = \frac{G_{SSN_m,SDN_m} P_{SSN_m}}{\sum_{j=1,j\neq m}^{M} G_{SSN_j,SDN_m} P_{SSN_j} + \sum_{l=1}^{L} G_{PT_l,SDN_m} P_{PT_l} + \eta_1}. \tag{12}$$

For the mth SR, the received signal at the mth SSN-SR link is

$$\begin{aligned} y_m^{SSN,SR} &= \sqrt{G_{SSN_m,SR_m}}\sqrt{P_{SSN_m}} z_m \\ &\quad + \sum_{j=1,j\neq m}^{M} \sqrt{G_{SSN_j,SR_m}}\sqrt{P_{SSN_j}} z_j \\ &\quad + \sum_{l=1}^{L} \sqrt{G_{PT_l,SR_m}}\sqrt{P_{PT_l}} x_l + w_2, \end{aligned} \tag{13}$$

where w_2 is the AWGN; power is η_2, with $\sum_{j=1,j\neq m}^{M} \sqrt{G_{SSN_j,SR_m}}\sqrt{P_{SSN_j}} z_j$ and $\sum_{l=1}^{L} \sqrt{G_{PT_l,SR_m}}\sqrt{P_{PT_l}} x_l$ as the interference

signals caused by the other SSNs and PTs at the mth SR. Therefore, the SINR of the mth SSN-SR link is

$$\gamma_m^{SSN,SR} = \frac{G_{SSN_m,SR_m}P_{SR_m}}{\sum_{j=1,j\neq m}^{M} G_{SSN_j,SR_m}P_{SSN_j} + \sum_{l=1}^{L} G_{PT_l,SR_m}P_{PT_l} + \eta_2}. \quad (14)$$

In Phase 3 of each time slot, each SR decodes information, and then recodes information, and sends it to its corresponding SDN. Therefore, the signal received at the mth SDN in the third part of the time slot will be

$$\begin{aligned} y_m^{SR,SDN} &= \sqrt{G_{SR_m,SDN_m}}\sqrt{P_{SR_m}}z'_m \\ &+ \sum_{j=1,j\neq m}^{M} \sqrt{G_{SR_j,SDN_m}}\sqrt{P_{SR_j}}z'_j \\ &+ \sum_{l=1}^{L} \sqrt{G_{PT_l,SDN_m}}\sqrt{P_{PT_l}}x_l + w_3 \end{aligned} \quad (15)$$

where w_3 is the AWGN; power is η_3, z'_m is the recoded symbol of z_m, and $\sum_{j=1,j\neq m}^{M} \sqrt{G_{SR_j,SDN_m}}\sqrt{P_{SR_j}}z_j$ and $\sum_{l=1}^{L} \sqrt{G_{PT_l,SDN_m}}\sqrt{P_{PT_l}}x_l$ are the interference signals created by the other SRs and PTs at the mth SDN, so the SINR of the mth SR-SDN link is

$$\gamma_m^{SR,SDN} = \frac{G_{SR_m,SDN_m}P_{SR_m}}{\sum_{j=1,j\neq m}^{M} G_{SR_j,SDN_m}P_{SR_j} + \sum_{l=1}^{L} G_{PT_l,SDN_m}P_{PT_l} + \eta_3}. \quad (16)$$

For the decode-and-forward (DF) relay protocol, the throughput of the mth secondary user is as follows:

$$\begin{aligned} R_m &= \frac{1-\alpha}{2} W \log_2(1+\gamma_m) \\ &= \frac{1-\alpha}{2} W \log_2(1+\min\{\gamma_m^{SSN,SR}, \gamma_m^{SSN,SDN} \\ &\quad + \gamma_m^{SR,SDN}\}) \\ &= \frac{1-\alpha}{2} W \min\{\log_2(1+\gamma_m^{SSN,SR}), \log_2(1+\gamma_m^{SSN,SDN} \\ &\quad + \gamma_m^{SR,SDN})\}, \end{aligned} \quad (17)$$

where W represents the bandwidth of the available channel, and γ_m is the end-to-end SINR of the mth SSN-SDN pair. Hence, the throughput of the secondary network is

$$\begin{aligned} R^{\text{total}} &= \sum_{m=1}^{M} R_m = \frac{1-\alpha}{2} W \sum_{m=1}^{M} \log_2(1+\gamma_m) \\ &= \frac{1-\alpha}{2} W \sum_{m=1}^{M} \min\{\log_2(1+\gamma_m^{SSN,SR}), \\ &\quad \log_2(1+\gamma_m^{SSN,SDN} + \gamma_m^{SR,SDN})\}. \end{aligned} \quad (18)$$

C. OPTIMIZATION PROBLEM

Following up on the system performance addressed above, our purpose is to maximize the throughput of the secondary network. Therefore, the optimization problem of maximal throughput can be formulated as (19), as shown at the top of the next page.

In (19), $\boldsymbol{r} = [r_1, r_2, \ldots, r_M]$ is the SR selection scheme. The first constraint and the second constraint are power constraints expressed in (9) and (10). For the third constraint, each SSN-SDN transmission pair should only select one SR to finish their transmission, and $r_m (m = 1, 2, \ldots, M)$ denotes that the SR is selected by the mth SSN-SDN transmission pair. Therefore, if the nth SR is selected by the mth SSN-SDN transmission pair, we make $r_m = n$. To optimize the joint multiple relay selection and time slot allocation is an NP-hard problem, so we propose a novel, intelligent, heuristic algorithm, the QSCA, to solve this problem.

IV. THROUGHPUT OPTIMIZATION BASED ON THE QUANTUM SINE COSINE ALGORITHM

In the CMRN, both the multiple relay selection scheme and the EH ratio should be considered in order to maximize throughput of the secondary network. Optimization of the multiple relay selection scheme is an integer problem. However, selection of the EH ratio is a continuous problem, so it is hard to easily apply a traditional, intelligent, heuristic algorithm to solve this problem. Therefore, we designed a novel QSCA to solve it.

A. QSCA FOR A HYBRID OPTIMIZATION PROBLEM

The QSCA is a new multi-agent optimization system that evolved from the sine cosine algorithm (SCA) [39] and the motivation of quantum calculation. In the $(M+1)$ dimensional space, there are H quantum individuals. Note: $(M+1)$ represents the number of dimensions for the optimization problem, and M represents the number of SSN-SDN transmission pairs. Each quantum individual consists of $(M+1)$ quantum bits. The hth $(h = 1, 2, \ldots, H)$ quantum individual of the tth generation can be represented by

$$\boldsymbol{x}_h^t = \begin{bmatrix} \alpha_{h1}^t, \alpha_{h2}^t, \ldots, \alpha_{hi}^t, \ldots, \alpha_{hM}^t, \alpha_{h(M+1)}^t \\ \beta_{h1}^t, \beta_{h2}^t, \ldots, \beta_{hi}^t, \ldots, \beta_{hM}^t, \beta_{h(M+1)}^t \end{bmatrix}, \quad (20)$$

where $i = 1, 2, \ldots, M+1$, $|\alpha_{hi}^t|^2 + |\beta_{hi}^t|^2 = 1$. We define $0 \le \alpha_{hi}^t \le 1$ and $0 \le \beta_{hi}^t \le 1$ to increase the efficiency of the QSCA, so $\beta_{hi}^t = \sqrt{1-(\alpha_{hi}^t)^2}$. Then, $\boldsymbol{x}_h^t$ can be simplified as follows:

$$\begin{aligned} \boldsymbol{x}_h^t &= \left[\alpha_{h1}^t, \alpha_{h2}^t, \ldots, \alpha_{hi}^t, \ldots, \alpha_{hM}^t, \alpha_{h(M+1)}^t\right] \\ &= \left[x_{h1}^t, x_{h2}^t, \ldots, x_{hi}^t, \ldots, x_{hM}^t, x_{h(M+1)}^t\right], \end{aligned} \quad (21)$$

where $i = 1, 2, \ldots, M+1$, and $0 \le x_{hi}^t \le 1$. Each x_{hi}^t is a quantum bit.

For each $\boldsymbol{x}_h^t$ in the whole population, the first M quantum bits are used to evolve the multiple relay selection scheme,

$$
\begin{aligned}
\text{maximize } f(\boldsymbol{r},\alpha) &= R^{\text{total}}(\boldsymbol{r},\alpha) \\
&= \frac{1-\alpha}{2} W \sum_{m=1}^{M} \min \left\{ \log_2 \left(1 + \frac{G_{SSN_m,SR_{rm}} P_{SR_{rm}}}{\sum\limits_{j=1,j\neq m}^{M} G_{SSN_j,SR_{rm}} P_{SSN_j} + \sum\limits_{l=1}^{L} G_{PT_l,SR_{rm}} P_{PT_l} + \eta_2} \right), \right. \\
&\quad \log_2 \left(1 + \frac{G_{SSN_m,SDN_m} P_{SSN_m}}{\sum\limits_{j=1,j\neq m}^{M} G_{SSN_j,SDN_m} P_{SSN_j} + \sum\limits_{l=1}^{L} G_{PT_l,SDN_m} P_{PT_l} + \eta_1} \right. \\
&\quad \left. \left. + \frac{G_{SR_{rm},SDN_m} P_{SR_{rm}}}{\sum\limits_{j=1,j\neq m}^{M} G_{SR_{r_j},SDN_m} P_{SR_{r_j}} + \sum\limits_{l=1}^{L} G_{PT_l,SDN_m} P_{PT_l} + \eta_3} \right) \right\} \\
\text{subject to } P_{SSN_m} &= \min \left(\frac{E_{SSN_m}}{(1-\alpha)T/2}, \frac{I_{\text{th}}}{M(\max(G_{SSN_m,PR_k}))} \right) \\
P_{SR_n} &= \min \left(\frac{E_{SR_n}}{(1-\alpha)T/2}, \frac{I_{\text{th}}}{M(\max(G_{SR_n,PR_k}))} \right) \\
r_m &\neq r_j, \quad \forall m \neq j \\
0 &\leq \alpha \leq 1
\end{aligned}
\tag{19}
$$

and the $(M+1)$th quantum bit is used to evolve the EH ratio. Since they are two different types of variable, hybrid evolution methods will be used. All the quantum individuals should be mapped to the definition domain, and the rule for mapping can be shown as follows:

$$
\begin{aligned}
\bar{x}_{hi}^{t} &= l_i + x_{hi}^{t}(u_i - l_i), \\
l_i &= \begin{cases} 1 & \text{if } i \neq M+1 \\ 0 & \text{if } i = M+1, \end{cases} \\
u_i &= \begin{cases} N & \text{if } i \neq M+1 \\ 1 & \text{if } i = M+1, \end{cases}
\end{aligned}
\tag{22}
$$

where $\bar{x}_{hi}^{t}$ is the mapping real state of x_{hi}^{t}, l_i is the lower bound of the ith dimensional variant, and u_i is the upper bound of the ith dimensional variant.

The optimal multiple relay selection is an integer optimization problem, so the first M quantum bits should be mapped from real number to integer. Since the optimal EH ratio is a continuous problem, the $(M+1)$th quantum bit keeps the original state. The mapping rule for each quantum bit is as follows:

$$
\bar{\bar{x}}_{hi}^{t} = \begin{cases} \text{round}(\bar{x}_{hi}^{t}) & \text{if } i = 1, 2, \ldots, M \\ \bar{x}_{hi}^{t} & \text{if } i = M+1 \end{cases}
\tag{23}
$$

where $\bar{\bar{x}}_{hi}^{t}$ is the integer state of x_{hi}^{t} and means rounding up to $\bar{x}_{hi}^{t}$, $\bar{\bar{\boldsymbol{x}}}_{h}^{t} = [\bar{\bar{x}}_{h1}^{t}, \bar{\bar{x}}_{h2}^{t}, \ldots, \bar{\bar{x}}_{h(M+1)}^{t}]$. The rounding function rounds up a real number to an integer.

The fitness of the hth quantum individual is computed by

$$
f(\bar{\bar{\boldsymbol{x}}}_{h}^{t+1}) = \begin{cases} f(\bar{\bar{\boldsymbol{x}}}_{h}^{t+1}), & \bar{\bar{x}}_{hi}^{t+1} \neq \bar{\bar{x}}_{hj}^{t+1} (\forall i \neq j,\ i,j = 1, 2, \ldots, M) \\ 0, & \text{else} \end{cases}
\tag{24}
$$

Since each SSN-SDN transmission pair can only select one SR, we should delete the unmatched solution. In (24) above, a penalty factor is used for removing incorrect solutions, i.e., if one solution cannot meet $\bar{\bar{x}}_{hi}^{t+1} \neq \bar{\bar{x}}_{hj}^{t+1} (\forall i \neq j, i, j = 1, 2, \ldots, M)$, its fitness should be calculated as zero, because two different SSN-SDN transmission pairs cannot use the same relay in our problem.

For each quantum individual, the evolutionary method is based on quantum rotation gate and quantum rotation angle. Until the tth generation, the global optimal quantum individual of the whole population is $\boldsymbol{p}_g^t = [p_{g1}^t, p_{g2}^t, \ldots, p_{g(M+1)}^t]$.

Because multiple relay selection and EH ratio are two distinct optimal problems, their evolutionary methods are different. For the hth $(h = 1, 2, \ldots, H)$ quantum individual, we first generate a uniform distributed random number, ξ_1, ranging from zero to one, and ξ_1 is used for selecting the evolutionary approach. When ξ_1 is less than 0.5, the ith $(i = 1, 2, \ldots, M+1)$ quantum rotation angle and the ith quantum bit are updated by

$$
\theta_{hi}^{t+1} = \begin{cases} c_1 \cdot \xi_2 \cdot \sin(\xi_3) \cdot (p_{gi}^{t} - x_{hi}^{t}) \text{ if } i \neq M+1 \\ c_2 \cdot \xi_2 \cdot \sin(\xi_4) \cdot (p_{gi}^{t} - x_{hi}^{t}) \text{ if } i = M+1 \end{cases}
\tag{25}
$$

$$
v_{hi}^{t+1} = \text{abs}(x_{hi}^{t} \cdot \cos\theta_{hi}^{t+1} + \sqrt{1 - (x_{hi}^{t})^2} \cdot \sin\theta_{hn}^{t+1}),
\tag{26}
$$

where $\xi_2 = 2 - 2 \cdot t/K$, in which K is the maximal iteration number. c_1 and c_2 are control coefficients which can set as constants. ξ_3 and ξ_4 are uniform distributed random numbers ranging from zero to 0.5π. The evolution method of sine allows for relocation of each quantum individual around the global optimal quantum individual, and increases the convergence speed.

When ξ_1 is not less than 0.5, each quantum individual will take another evolutionary rule, and the ith quantum rotation angle and the ith quantum bit for the hth quantum individual are updated by

$$\theta_{hi}^{t+1} = \begin{cases} c_3 \cdot \cos(\xi_3) \cdot (x_{ai}^t - x_{hi}^t) \text{ if } i \neq M+1 \\ c_4 \cdot \cos(\xi_4) \cdot (x_{ai}^t - x_{hi}^t) \text{ if } i = M+1 \end{cases} \quad (27)$$

$$v_{hi}^{t+1} = \text{abs}(x_{hi}^t \cdot \cos\theta_{hi}^{t+1} + \sqrt{1-(x_{hi}^t)^2} \cdot \sin\theta_{hn}^{t+1}), \quad (28)$$

where $a \in \{1, 2, \ldots, H\}$ is a random integer, and the cosine evolution rule can increase the population diversity. c_3 and c_4 are control coefficients.

The quantum individual, $\boldsymbol{v}_h^{t+1}$ $(h = 1, 2, \ldots, H)$, is mapped to integer number vector $\bar{\bar{\boldsymbol{v}}}_h^{t+1}$. Then, the fitness of $\bar{\bar{\boldsymbol{v}}}_h^{t+1}$ is computed by the fitness function. If the fitness of $\bar{\bar{\boldsymbol{v}}}_h^{t+1}$ is greater than that of $\bar{\bar{\boldsymbol{x}}}_h^t$, then $x_h^{t+1} = \boldsymbol{v}_h^{t+1}$; otherwise, $\boldsymbol{x}_h^{t+1} = \boldsymbol{x}_h^t$. Finally, the best quantum individual of the current generation is used to update the global optimal quantum individual.

B. JOINT MULTIPLE RELAY SELECTION AND TIME SLOT ALLOCATION PROCESS BASED ON QSCA

The QSCA is able to optimize the secondary users' joint multiple relay selection and time slot allocation problem in a CMRN. The fitness function of QSCA is set as $f(\bar{\bar{\boldsymbol{x}}}_h^t) = \begin{cases} R^{\text{total}}(\bar{\bar{\boldsymbol{x}}}_h^t), & \text{satisfy constraint condition} \\ 0, & \text{else} \end{cases}$. The fitness of each quantum individual in the population is calculated by this fitness function. The mapping state of each quantum individual is corresponding to the multiple relay selection and EH ratio which are to be optimized. The joint multiple relay selection and time slot allocation process based on QSCA is presented in Algorithm 1.

Algorithm 1 Joint Multiple Relay Selection and Time Slot Allocation Process Based on QSCA

1 Input system parameters of CMRN with EH;
2 Initialize parameter settings and the initial population of QSCA;
3 $t = 1$ // the first iteration;
4 Map each quantum individual to the definition domain according to (22) and (23);
5 Calculate the fitness value of each quantum individual according to the fitness function (24);
6 Obtain the global optimal quantum individual $\boldsymbol{p}_g^t$;
7 while $t \leq t_{\max}$
8 **if** $\xi_1 < 0.5$
9 Update the quantum individual by (25) and (26)
10 **else**
11 Update the quantum individual by (27) and (28)
12 end if
13 Map each quantum individual and calculate the fitness;
14 Update the quantum individuals and the global optimal quantum individual according to the fitness;
15 Set $t = t + 1$;
17 end while
18 Obtain the optimal joint multiple relay selection and EH ratio result after K iterations;
19 Output: The optimal joint multiple relay selection and EH ratio result.

V. SIMULATION RESULTS AND ANALYSIS

Simulation results are presented here from examining the throughput of the secondary network with EH. For the first part, the proposed QSCA is compared with other existing intelligent algorithms. Actually, there are no existing intelligent algorithms that can solve the proposed joint multiple relay selection and time slot allocation problem. Nevertheless, to show the superiority of our proposed QSCA, we will compare it to other classic algorithms for solving general optimal problems. In the second part, we compare the simulation results for throughput under our proposed QSCA to the scheme introduced in [26]. In the third part, we show the impact on the secondary network based on different system parameters. In this simulation, bandwidth is 10 MHz, and β is equal to 3. All the PTs are distributed randomly in a circle with a radius of 2 where the center is at (5, 20). The center of each PR is (25, 20), and each PR is located randomly around the center within a radius of 2. Each SSN and SDN are generated in two different circles with centers at (0, 0) and (30, 0). The radius of each pair of circles is 5. Then, N SRs are generated in a circle with a radius of 5, and the center of the circle is at (15, 0). The EH rate of each SSN is the same as the rate for each SR. In the simulation, $I_{\text{th}} = 8 \times 10^{-3}$. Other simulation parameters are shown in TABLE 2.

A. NUMERICAL PERFORMANCE COMPARISON VS. EXISTING INTELLIGENT ALGORITHMS

We show numerical simulation results for the throughput of the secondary network under the proposed QSCA and under existing intelligent algorithms. Actually, there are no existing intelligent algorithms for solving our proposed problem model. For verifying the performance of the QSCA, we apply existing intelligent algorithms for solving the proposed optimization problem. They are the differential evolutionary algorithm (DEA) and the SCA. The maximal iterations were set to 1500, and the population size, H, was 20 for the QSCA, the DEA, and the SCA. The parameter settings of the SCA and the parameter settings for DEA came from [39] and [40], respectively.

Fig. 3 shows convergence performance results of the proposed QSCA and two existing intelligent algorithms

TABLE 2. Main simulation parameters.

Parameter	Value
System bandwidth	10MHz
Path loss factor	3
Interference threshold of PUs	8×10^{-3}
Power of the AWGN at all nodes	10^{-3} W
Number of PT-PR transmission pairs	5
Number of SSN-SDN transmission pairs	10
Power of all PTs	2W
Number of SRs	20
Maximal iterations	1500
Population size	20
Control coefficient c_1	0.8
Control coefficient c_2	0.3
Control coefficient c_3	1
Control coefficient c_4	0.3

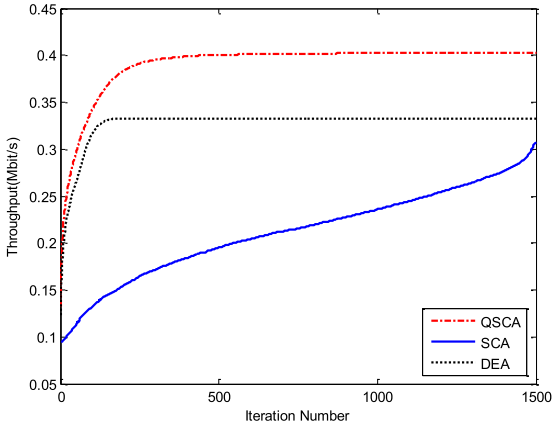

FIGURE 3. Convergence performance comparison of the proposed QSCA vs. existing intelligent algorithms.

(the SCA and the DEA) with 20 SRs. The maximum number of iterations was 1500 for a clear comparison. In this simulation, $Y_{SSN} = 20$, and $Y_{SR} = 12$. The simulation results show that the QSCA can get better performance than the DEA and SCA for throughput in the secondary network. It is clear that the performance of the QSCA is superior to the DEA and SCA. The proposed QSCA is a combination of the quantum computing theory and the sine cosine algorithm. In the traditional SCA, the search solution is to find the optimal solution inside the search set from certain updating equations. The SCA is able to find the approximate region for a solution in the search set. However, the traditional SCA has the shortcomings of randomness, local convergence, and slow convergence speed. Therefore, the SCA cannot provide good performance when solving the problem model proposed in this paper. For QSCA, the evolution method of sine allows for relocation of each quantum individual to obtain the global optimal quantum individual, and increases the convergence speed. Besides, the designed cosine evolution rule can increase the population diversity of QSCA. Compared with the SCA, the QSCA has the merits of both the sine cosine theory and quantum computing, which can improve the convergence speed and population diversity, so it is easy to attain good performance. When compared with other intelligent algorithms, the SCA can provide good performance. Due to the fact that the QSCA combines two evolution methods, the speed of convergence and the diversity of the population are better than with a traditional intelligent algorithm. In summary, it is easy for the QSCA to mitigate the shortcomings of the traditional algorithms and provide good performance.

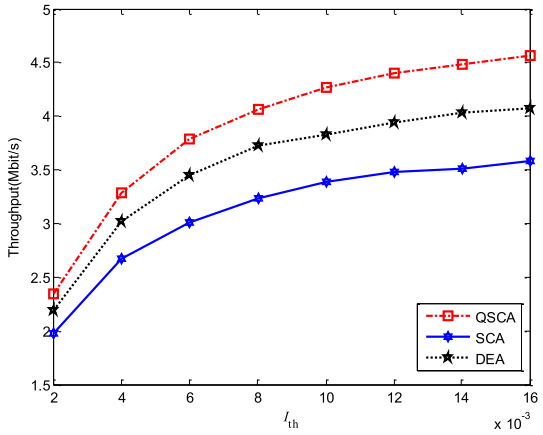

FIGURE 4. Throughput of the proposed QSCA vs. existing intelligent algorithms at different I_{th} values.

Fig. 4 considers the case where I_{th} varies from 2×10^{-3} to 1.6×10^{-2}. In the simulation, $Y_{SSN} = 20$, and $Y_{SR} = 20$. From the simulation results, we can see that as I_{th} increases, the throughput becomes larger and larger. It is easy to understand, because when I_{th} values are large, the SSNs and SRs are permitted to transmit at a high power, so the secondary network can make use of greater energy. Then, the throughput becomes larger. The simulation results show that the QSCA can provide better performance, compared with the SCA and DEA intelligent algorithms when we consider threshold value I_{th}.

Fig. 5 presents the throughput while the number of PT-PR transmission pairs varies from 2 to 16. In the simulation, $Y_{SSN} = 20$, and $Y_{SR} = 20$. The secondary network's throughput decreases when the number of PT-PR transmission pairs increases. That is because when the number of PT-PR transmission pairs becomes larger, it will have two kinds of impact on the secondary network. First, more PTs will cause more interference with the SRs and SDNs, and then, the SINR of the SSNs and SRs will become smaller than before. Second, when the number of PRs becomes larger, it is more possible that the SSNs and SRs will have an impact on a certain PT. Therefore, the power of the SSNs and SRs will become smaller than in situations when the number of PRs is small. For these two reasons, we get the simulation results mentioned above. From the simulation results, the QSCA

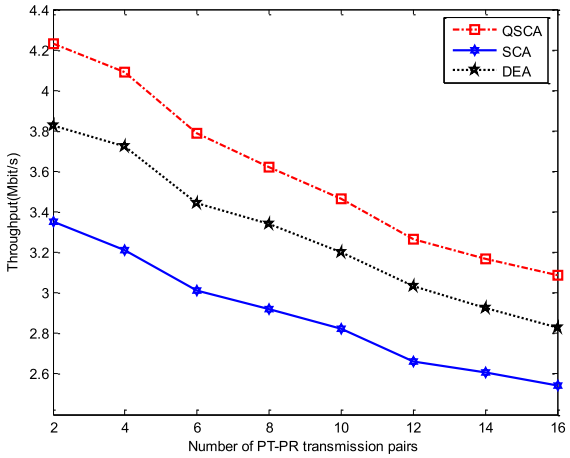

FIGURE 5. Throughput of the proposed QSCA vs. existing intelligent algorithms with different numbers of PT-PR transmission pairs.

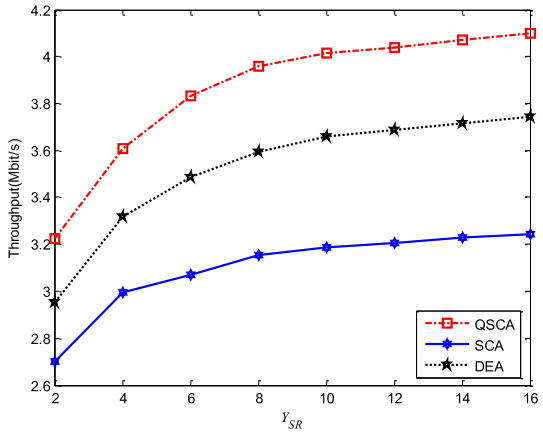

FIGURE 6. Throughput of the proposed QSCA vs. existing intelligent algorithms at different Y_{SR} values.

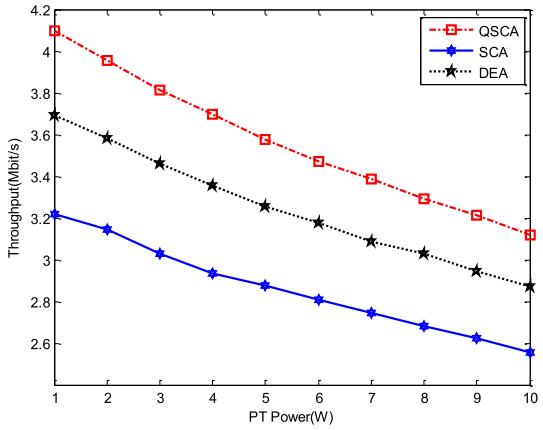

FIGURE 7. Throughput of the proposed QSCA vs. existing intelligent algorithms and different PT power levels.

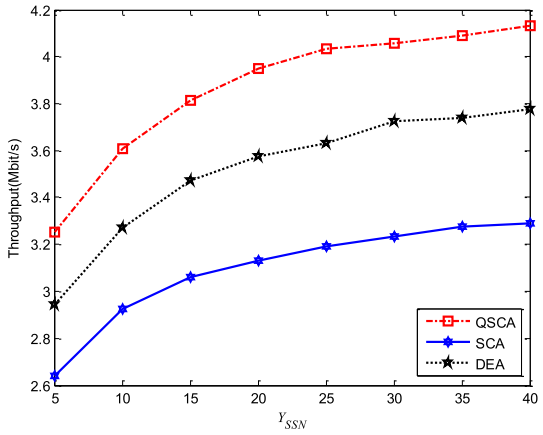

FIGURE 8. Throughput of the proposed QSCA vs. existing intelligent algorithms at different Y_{SSN} levels.

can provide better performance, compared with the SCA and DEA.

Fig. 6 illustrates the secondary network's throughput for various Y_{SR} levels. In the simulation, $Y_{SSN} = 20$. The simulation results compare the performance of the QSCA, SCA, and DEA. The QSCA can provide the best performance among the three schemes. From the simulation results, it is easy draw the conclusion that as Y_{SR} increases, throughput becomes larger and larger. That is because a larger Y_{SR} will bring SRs more power for cooperative transmission. However, due to the constraints on the primary network, even if more energy is harvested, it is hard to fully utilize it. Therefore, the increasing speed of the throughput is lower and lower.

Fig. 7 considers the impact on the secondary network of PT power. In the simulation, $Y_{SSN} = 20$, and $Y_{SR} = 20$. The power of each PT varies from 1 W to 10 W. It is easy to see that throughput decreases as PT power increases due to the fact that more PT power will cause more interference with the SSNs and SRs. Compared with the SCA and the DEA, the QSCA can provide better performance at different PT power levels.

Fig. 8 is the simulation results from different Y_{SSN} levels. In the simulation, $Y_{SR} = 30$, Y_{SSN} varies from 5 to 40, and throughput increases as Y_{SSN} becomes larger and larger. The larger Y_{SSN} will bring more energy to the SSN for transmitting information. By comparing it with the SCA and the DEA, the QSCA can provide the best simulation results. So, this shows good performance from the QSCA we have proposed.

In Fig. 9, different numbers of SRs are considered. In the simulation, $Y_{SSN} = 12$, and $Y_{SR} = 12$. For a certain situation in the secondary network, a higher number of SRs can improve the throughput of the secondary network. More SRs can provide more choices to transmit information in the secondary network. Therefore, when the number of SRs increases, throughput gains better performance. Also, we can see that the proposed QSCA can obtain a better outcome when compared with the SCA and the DEA. All the simulation results show the advantages of the QSCA.

B. COMPARISON OF QSCA AND A TRADITIONAL SCHEME

In this section, the simulation results for throughput with the QSCA and the scheme in [26] are presented. Actually, there is no way for the energy harvesting-information

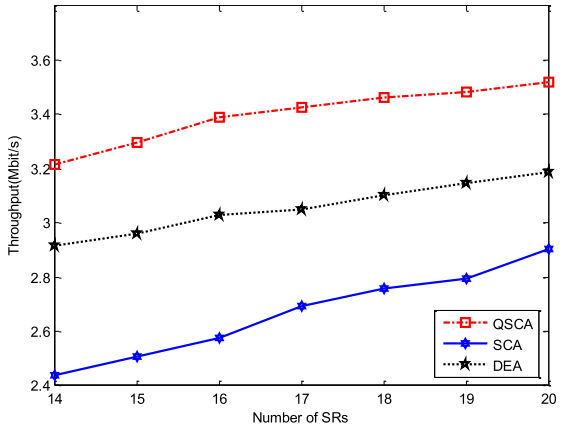

FIGURE 9. Throughput of the proposed QSCA vs. existing intelligent algorithms and different numbers of SRs.

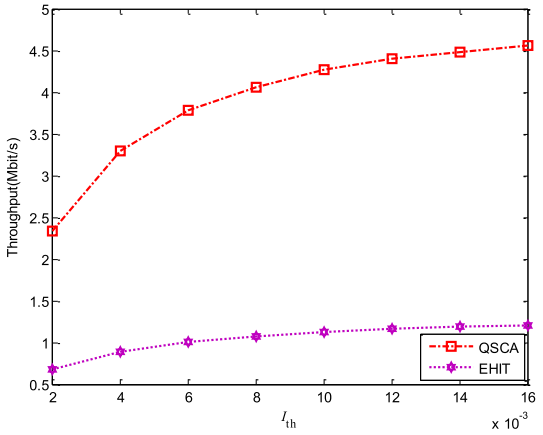

FIGURE 10. Throughput of the proposed QSCA vs. EHIT and different I_{th} values.

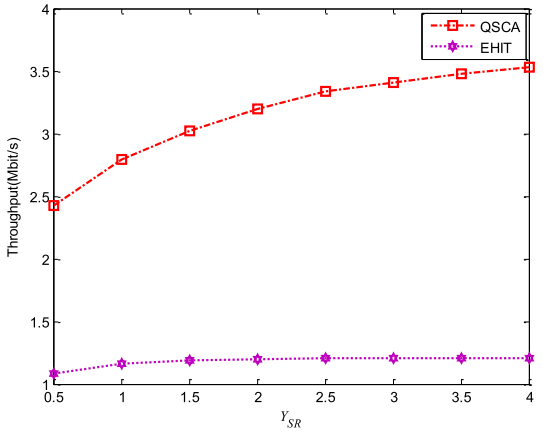

FIGURE 11. Throughput of the proposed QSCA vs. EHIT and different Y_{SR} values.

transmission (EHIT) scheme in [26] to process relay selection, because the authors only proposed a method of setting the EH ratio. Therefore, we select relays randomly for the [26].

Fig. 10 to Fig. 12 compare the performance of QSCA and EHIT from three aspects: I_{th}, Y_{SR}, and PT power. In [26]

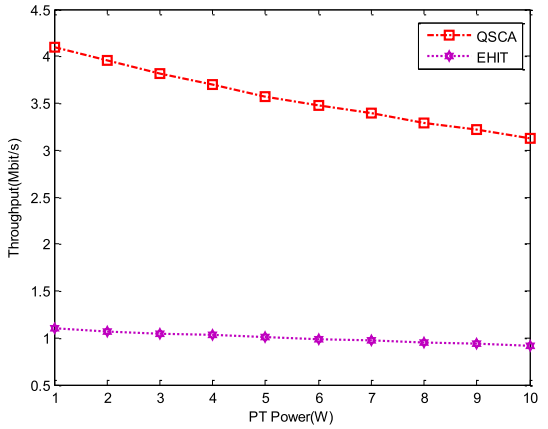

FIGURE 12. Throughput of the proposed QSCA vs. EHIT and different PT power levels.

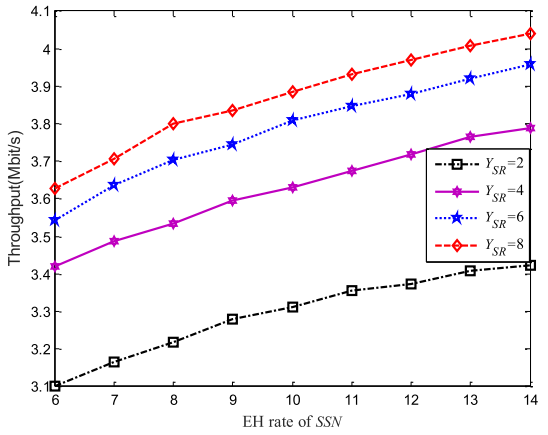

FIGURE 13. Throughput of different Y_{SSN} and Y_{SR} values.

Liu *et al.* set the EH ratio at a fixed value, i.e., $\alpha = 0.5$. Besides that, there is no efficient multiple relay selection scheme in [26]. All the simulation results show that the QSCA is better than EHIT under different simulation sceneries. They also show the effectiveness of the proposed method.

C. SIMULATIONS OF DIFFERENT PARAMETERS BASED ON THE QSCA FOR A CMRN

For this section, we will show the simulation results of different parameters, and the impact on the secondary network of different parameters will be discussed.

Fig. 13 shows the throughput when $Y_{SR} = 2$, $Y_{SR} = 4$, $Y_{SR} = 6$, and $Y_{SR} = 8$. The EH rate of an SSN varies from 6 to 14. From the simulation results, we can see that a larger Y_{SR} can increase the secondary network's throughput. Due to the fact that a larger Y_{SR} can provide more energy to the SRs for transmission, the performance of the secondary network can be improved by increasing Y_{SR}. Also, the larger the Y_{SSN} value, the more energy is able to be utilized for transmission. Therefore, boosting Y_{SSN} and Y_{SR} can improve the performance of the secondary network.

Fig. 14 shows the situations with different PT power and I_{th} levels in the secondary network. The PT power

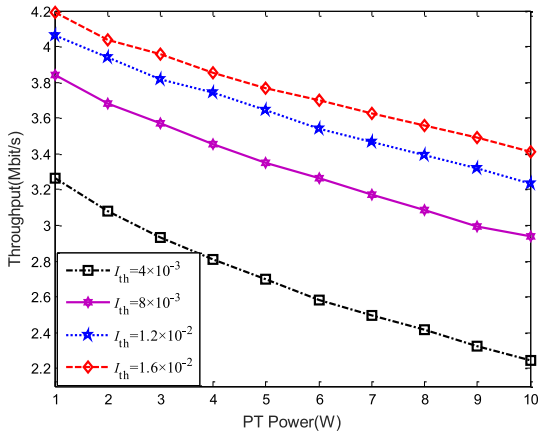

FIGURE 14. Throughput of different PT power and I_{th} levels.

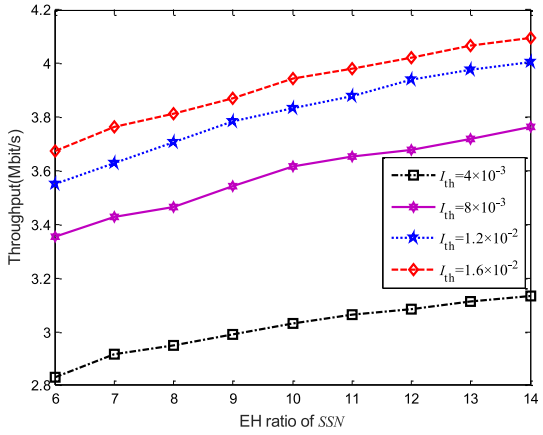

FIGURE 15. Throughput of different Y_{SSN} and I_{th} levels.

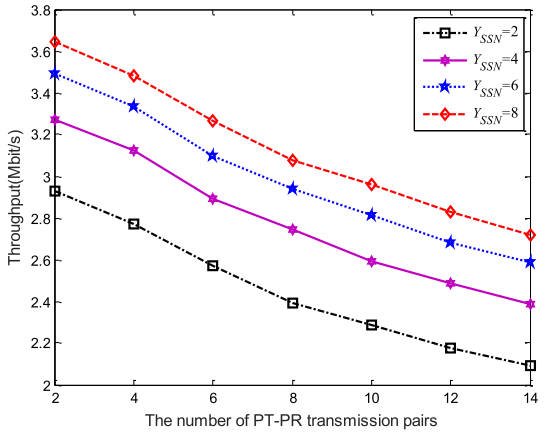

FIGURE 16. Throughput of different numbers of PT-PR transmission pairs and levels for Y_{SSN}.

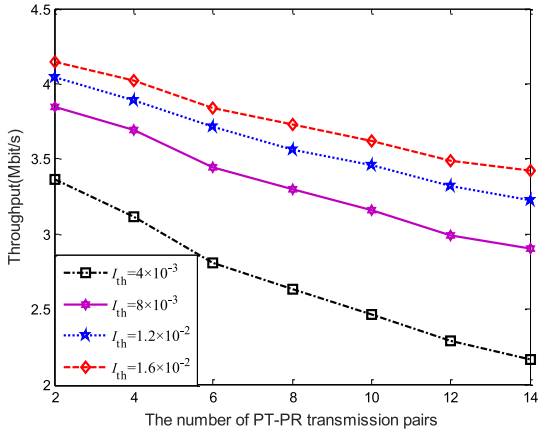

FIGURE 17. Throughput of different numbers of PT-PR transmission pairs and different levels for I_{th}.

varies from 1 W to 10 W. In the simulation, values are $Y_{SSN} = 12$, $Y_{SR} = 12$, and I_{th} is 4×10^{-3}, 8×10^{-3}, 1.2×10^{-2}, and 1.6×10^{-2}. For the secondary network, the PT-PR transmission pairs will cause interference with the SRs and SDNs. The increase in PT power will bring stronger interference into the secondary network. Therefore, the secondary network's throughput becomes smaller and smaller while PT power increases. Besides, from the simulation results, we can see the secondary network's throughput is increasing while I_{th} increases.

In Fig. 15, the impact of different Y_{SSN} and I_{th} levels on the secondary network is studied. In the simulation, $Y_{SR} = 10$. We increase Y_{SSN} from 6 to 14, while I_{th} is 4×10^{-3}, 8×10^{-3}, 1.2×10^{-2} and 1.6×10^{-2}. Higher Y_{SSN} and I_{th} levels are both able to improve the performance of the secondary network. The secondary network's throughput can be improved by increasing Y_{SSN}. For a certain Y_{SSN}, a higher I_{th} can make use of the harvested energy better than a lower I_{th}, and that is because the PUs allow the secondary network to transmit at a higher power when I_{th} increases.

Fig. 16 is the simulation results with which we consider different numbers of PT-PR transmission pairs and different levels for Y_{SSN}. In the simulation, Y_{SSN} is equal to 2, 4, 6, and 8, and $Y_{SR} = 30$. The number of PT-PR transmission pairs varies from 2 to 14. As more PT-PR transmission pairs communicate through the primary network, the throughput of the secondary network decreases. The higher Y_{SSN} can provide more energy to the secondary network, and the throughput increases with a higher Y_{SSN}.

In Fig. 17, we consider the influence on throughput of I_{th} and different numbers of PT-PR transmission pairs. In the simulation, $Y_{SSN} = 12$, and $Y_{SR} = 12$. More PT-PR transmission pairs cause more interference with the secondary network, and each secondary user's SINR becomes lower. Therefore, the secondary network's throughput decreases while the number of PT-PR transmission pairs increases. For a certain number of PT-PR transmission pairs, the higher I_{th} can enhance throughput.

To see the relationship of the two different parameters more clearly, we show the simulation results another way. In the simulation, $Y_{SR} = 12$. For Fig. 18, two parameters (PT power and Y_{SSN}) are studied. PT power varies from 1 W to 10 W, and Y_{SSN} varies from 4 to 16. For the secondary network, the higher PT power is harmful to the secondary network, whereas the higher Y_{SSN} is beneficial to the secondary network.

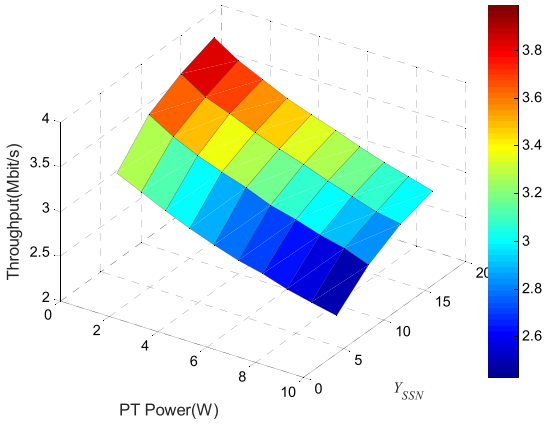

FIGURE 18. Throughput of different levels for PT power and Y_{SSN}.

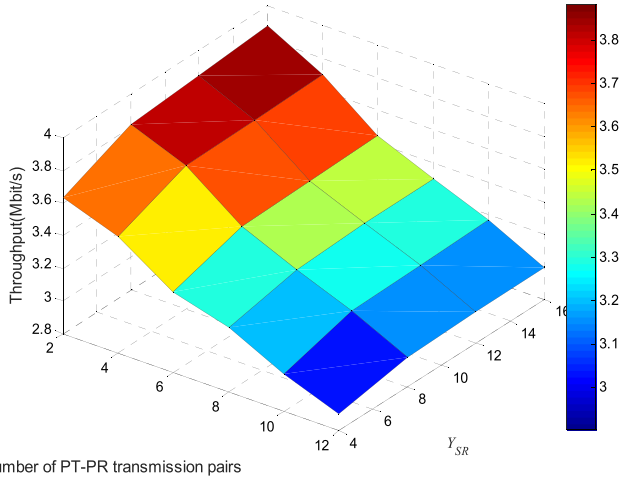

FIGURE 19. Throughput from different numbers of PT-PR transmission pairs and different levels for Y_{SR}.

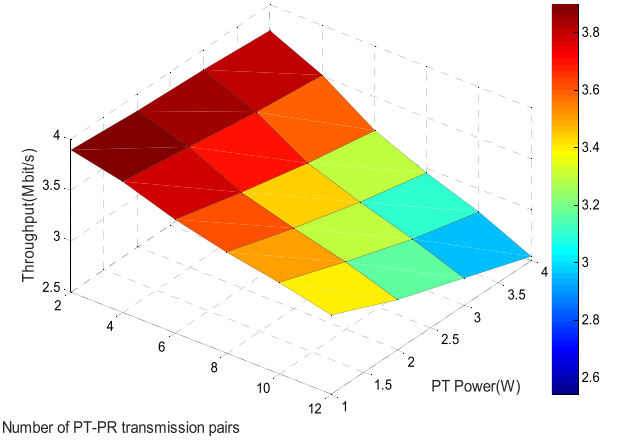

FIGURE 20. Throughput from different numbers of PT-PR transmission pairs and different PT power levels.

Fig. 19 shows the simulation results for throughput based on different numbers of PT-PR transmission pairs and different levels for Y_{SR}. In the simulation, $Y_{SSN} = 12$, and Y_{SR} is 4, 8, 12, and 16. The impact of Y_{SR} and the number of PT-PR transmission pairs on the secondary network is clear. A higher Y_{SR} and fewer PT-PR transmission pairs enhance the performance of the secondary network.

Fig. 20 is the simulation results of two system parameters: PT power and the number of PT-PR transmission pairs. In the simulation, $Y_{SSN} = 12$, and $Y_{SR} = 12$. It is easy to see that both the larger number of PT-PR transmission pairs and higher power are harmful to the secondary network. Reducing them in communications networks is a meaningful thing.

VI. CONCLUSION

In this paper, we proposed a new CMRN with EH. To further study the performance of a CMRN, we derived an analytical expression for the throughput of the secondary network. To maximize throughput and then get the optimal multiple relay selection scheme and EH ratio, we proposed a new algorithm: the QSCA. The QSCA has the merits of both sine cosine evolution approach and quantum computing theory, which can improve the convergence speed and population diversity. Compared with traditional algorithms, the proposed QSCA scheme provides good performance under different simulation sceneries. Besides, the simulation results also validate the QSCA can obtain an efficient multiple relay selection scheme and EH ratio under different system parameters. In the future, this work will be be incorporated with some other cognitive communication scenarios, such as smart grid, A-IoT, and Industry 4.0, in which CRNs and EH play important roles.

ABBREVIATIONS

AWGN:	Additive white Gaussian noise;
CCI:	Co-channel interference;
CMRN:	Cognitive Multi-user relay network;
CRN:	Cognitive relay network;
CSI:	Channel state information;
DEA:	Differential evolutionary algorithm;
DF:	Decode-and-forward;
EH:	Energy harvesting;
MRC:	Maximum ratio combining;
PR:	Primary receiver;
PT:	Primary transmitter;
PU:	Primary user;
QSCA:	Quantum sine cosine algorithm;
SCA:	Sine cosine algorithm;
SDN:	Secondary destination node;
SINR:	Signal-to-interference-plus-noise ratio;
SR:	Secondary relay;
SSN:	Secondary source node;
SU:	Secondary user.

REFERENCES

[1] N. I. Miridakis, T. A. Tsiftsis, G. C. Alexandropoulos, and M. Debbah, "Green cognitive relaying: Opportunistically switching between data transmission and energy harvesting," *IEEE J. Sel. Areas Commun.*, vol. 34, no. 12, pp. 3725–3738, Dec. 2016.

[2] P. Gandotra, R. K. Jha, and S. Jain, "Green communication in next generation cellular networks: A survey," *IEEE Access*, vol. 5, pp. 11727–11758, 2017.

[3] H. Gao, Y. Su, S. Zhang, and M. Diao, "Antenna selection and power allocation design for 5G massive MIMO uplink networks," *China Commun.*, vol. 16, no. 4, pp. 1–15, Apr. 2019.
[4] X. Lu, P. Wang, D. Niyato, D. I. Kim, and Z. Han, "Wireless networks with RF energy harvesting: A contemporary survey," *IEEE Commun. Surveys Tuts.*, vol. 17, no. 2, pp. 757–789, 2nd Quart., 2015.
[5] D. T. Hoang, D. Niyato, P. Wang, D. I. Kim, and Z. Han, "Ambient backscatter: A new approach to improve network performance for RF-powered cognitive radio networks," *IEEE Trans. Commun.*, vol. 65, no. 9, pp. 3659–3674, Sep. 2017.
[6] A. Mukherjee, T. Acharya, and M. R. A. Khandaker, "Outage analysis for SWIPT-enabled two-way cognitive cooperative communications," *IEEE Trans. Veh. Technol.*, vol. 67, no. 9, pp. 9032–9036, Sep. 2018.
[7] H. Gao, W. Ejaz, and M. Jo, "Cooperative wireless energy harvesting and spectrum sharing in 5G networks," *IEEE Access*, vol. 4, pp. 3647–3658, 2016.
[8] S. Yin, E. Zhang, Z. Qu, L. Yin, and S. Li, "Optimal cooperation strategy in cognitive radio systems with energy harvesting," *IEEE Trans. Wireless Commun.*, vol. 13, no. 9, pp. 4693–4707, Sep. 2014.
[9] Q. Wu, M. Tao, D. W. K. Ng, W. Chen, and R. Schober, "Energy-efficient resource allocation for wireless powered communication networks," *IEEE Trans. Wireless Commun.*, vol. 15, no. 3, pp. 2312–2327, Mar. 2016.
[10] J. Guo, S. Durrani, and X. Zhou, "Performance analysis of arbitrarily-shaped underlay cognitive networks: Effects of secondary user activity protocols," *IEEE Trans. Commun.*, vol. 63, no. 2, pp. 376–389, Feb. 2015.
[11] M. Choi, J. Park, and S. Choi, "Low complexity multiple relay selection scheme for cognitive relay networks," in *Proc. IEEE Veh. Technol. Conf. (VTC Fall)*, San Francisco, CA, USA, Sep. 2011, pp. 1–5.
[12] T. Q. Duong, P. L. Yeoh, V. N. Q. Bao, M. Elkashlan, and N. Yang, "Cognitive relay networks with multiple primary transceivers under spectrum-sharing," *IEEE Signal Process. Lett.*, vol. 19, no. 11, pp. 741–744, Nov. 2012.
[13] C. Xu, M. Zheng, W. Liang, H. Yu, and Y.-C. Liang, "Outage performance of underlay multihop cognitive relay networks with energy harvesting," *IEEE Commun. Lett.*, vol. 20, no. 6, pp. 1148–1151, Jun. 2016.
[14] S. S. Kalamkar and A. Banerjee, "Secure communication via a wireless energy harvesting untrusted relay," *IEEE Trans. Veh. Technol.*, vol. 66, no. 3, pp. 2199–2213, Mar. 2017.
[15] W. Lu, T. Nan, Y. Gong, M. Qin, X. Liu, Z. Xu, and Z. Na, "Joint resource allocation for wireless energy harvesting enabled cognitive sensor networks," *IEEE Access*, vol. 6, pp. 22480–22488, 2018.
[16] C. K. Ho and R. Zhang, "Optimal energy allocation for wireless communications with energy harvesting constraints," *IEEE Trans. Signal Process.*, vol. 60, no. 9, pp. 4808–4818, Sep. 2012.
[17] O. Ozel, K. Shahzad, and S. Ulukus, "Optimal energy allocation for energy harvesting transmitters with hybrid energy storage and processing cost," *IEEE Trans. Signal Process.*, vol. 62, no. 12, pp. 3232–3245, Jun. 2014.
[18] G. Han, J.-K. Zhang, and X. Mu, "Joint optimization of energy harvesting and detection threshold for energy harvesting cognitive radio networks," *IEEE Access*, vol. 4, pp. 7212–7222, 2016.
[19] P. Maji, S. D. Roy, and S. Kundu, "Secrecy outage analysis in a hybrid cognitive relay network with energy harvesting," *Int. J. Commun. Syst.*, vol. 30, no. 10, Jul. 2017, Art. no. e3228.
[20] F. Yao, H. Wu, Y. Chen, Y. Liu, and T. Liang, "Cluster-based collaborative spectrum sensing for energy harvesting cognitive wireless communication network," *IEEE Access*, vol. 5, pp. 9266–9276, 2017.
[21] Z. Yan, S. Chen, X. Zhang, and H.-L. Liu, "Outage performance analysis of wireless energy harvesting relay-assisted random underlay cognitive networks," *IEEE Internet Things J.*, vol. 5, no. 4, pp. 2691–2699, Aug. 2018.
[22] S. Singh, S. Modem, and S. Prakriya, "Optimization of cognitive two-way networks with energy harvesting relays," *IEEE Commun. Lett.*, vol. 21, no. 6, pp. 1381–1384, Jun. 2017.
[23] Y. Al-Eryani, "Exact performance of wireless-powered communications with maximum ratio combining," in *Wireless Personal Communications*. Berlin, Germany: Springer, to be published. doi: 10.1007/s11277-019-06489-6.
[24] A. Bhowmick, S. D. Roy, and S. Kundu, "Throughput of a cognitive radio network with energy-harvesting based on primary user signal," *IEEE Wireless Commun. Lett.*, vol. 5, no. 2, pp. 136–139, Apr. 2016.
[25] Z. Wang, Z. Chen, B. Xia, L. Luo, and J. Zhou, "Cognitive relay networks with energy harvesting and information transfer: Design, analysis, and optimization," *IEEE Trans. Wireless Commun.*, vol. 15, no. 4, pp. 2562–2576, Apr. 2016.
[26] Y. Liu, S. A. Mousavifar, Y. Deng, C. Leung, and M. Elkashlan, "Wireless energy harvesting in a cognitive relay network," *IEEE Trans. Wireless Commun.*, vol. 15, no. 4, pp. 2498–2508, Apr. 2016.
[27] N.-P. Nguyen, T. Q. Duong, H. Q. Ngo, Z. Hadzi-Velkov, and L. Shu, "Secure 5G wireless communications: A joint relay selection and wireless power transfer approach," *IEEE Access*, vol. 4, pp. 3349–3359, 2016.
[28] Z. Wang, Z. Chen, L. Luo, Z. Hu, B. Xia, and H. Liu, "Outage analysis of cognitive relay networks with energy harvesting and information transfer," in *Proc. IEEE Int. Conf. Commun. (ICC)*, Sydney, NSW, Australia, Jun. 2014, pp. 4348–4353.
[29] Q. Li, S. J. Feng, A. Pandharipande, X. Ge, Q. Ni, and J. Zhang, "Wireless-powered cooperative multi-relay systems with relay selection," *IEEE Access*, vol. 5, pp. 19058–19071, 2017.
[30] A. Zappone, S. Atapattu, M. Di Renzo, J. Evans, and M. Debbah, "Energy-efficient relay assignment and power control in multi-user and multi-relay networks," *IEEE Wireless Commun. Lett.*, vol. 7, no. 6, pp. 1070–1073, Dec. 2018.
[31] C. Esli and A. Wittneben, "A hierarchical AF protocol for distributed orthogonalization in multiuser relay networks," *IEEE Trans. Veh. Technol.*, vol. 59, no. 8, pp. 3902–3916, Oct. 2010.
[32] S. Sharma, Y. Shi, Y. T. Hou, and S. Kompella, "An optimal algorithm for relay node assignment in cooperative ad hoc networks," *IEEE/ACM Trans. Netw.*, vol. 19, no. 3, pp. 879–892, Jun. 2011.
[33] S. Atapattu, Y. Jing, H. Jiang, and C. Tellambura, "Relay selection and performance analysis in multiple-user networks," *IEEE J. Sel. Areas Commun.*, vol. 31, no. 8, pp. 1517–1529, Aug. 2013.
[34] K. Singh, A. Gupta, and T. Ratnarajah, "Energy efficient resource allocation for multiuser relay networks," *IEEE Trans. Wireless Commun.*, vol. 16, no. 2, pp. 1218–1235, Feb. 2017.
[35] J. Ho and M. Jo, "Offloading wireless energy harvesting for IoT devices on unlicensed bands," *IEEE Internet Things*, vol. 6, no. 2, pp. 3663–3675, Apr. 2019.
[36] K. Singh, A. Gupta, and T. Ratnarajah, "QoS-driven energy-efficient resource allocation in multiuser amplify-and-forward relay networks," *IEEE Trans. Signal Inf. Process. Netw.*, vol. 3, no. 4, pp. 771–786, Dec. 2017.
[37] S. Luo, R. Zhang, and T. J. Lim, "Optimal save-then-transmit protocol for energy harvesting wireless transmitters," *IEEE Trans. Wireless Commun.*, vol. 12, no. 3, pp. 1196–1207, Mar. 2013.
[38] O. Elnahas, M. Elsabrouty, O. Muta, and H. Furukawa, "Game theoretic approaches for cooperative spectrum sensing in energy-harvesting cognitive radio networks," *IEEE Access*, vol. 6, pp. 11086–11100, 2018.
[39] S. Mirjalili, "SCA: A sine cosine algorithm for solving optimization problems," *Knowl. Based Syst.*, vol. 96, pp. 120–133, Mar. 2016.
[40] R. Storn and K. Price, "Differential evolution–a simple and efficient heuristic for global optimization over continuous spaces," *J. Global Optim.*, vol. 11, no. 4, pp. 341–359, Dec. 1997.

HONGYUAN GAO received the Ph.D. degree from the Department of Communication and Information Systems, College of Information and Communication Engineering, Harbin Engineering University, China, in 2010. He was a Visiting Research Professor with the Department of Computer and Information Science, Korea University, Sejong City, South Korea, from 2015 to 2016, under the supervision of Prof. M. Jo. He is currently an Associate Professor with the College of Information and Communication Engineering, Harbin Engineering University, China. His current research interests include wireless energy harvesting communications, intelligent computing, artificial intelligence, radio signal recognition and classification, array signal processing, cognitive radio, HetNets in 5G, communication theory, image processing, and massive MIMO.

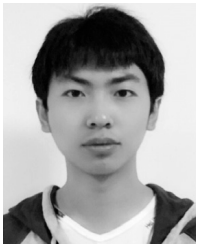

SHIBO ZHANG received the B.E. degree in electronic information engineering from Harbin Engineering University, Harbin, China, in June 2016, where he is currently pursuing the Ph.D. degree.

His current research interests include fog computing, cognitive relays, energy harvesting, heterogeneous networks, device-to-device communications, the Internet of Things, and future radio networks.

YUMENG SU received the B.E. degree in electronic information engineering from Harbin Engineering University, Harbin, China, in June 2016, where she is currently pursuing the Ph.D. degree.

Her current research interests include intelligent computing, relay selection, power allocation, massive MIMO, secure communications, co-frequency co-time full duplex systems, and beyond 5G technologies.

MING DIAO was born in 1960. He received the B.E. and M.E. degree from Harbin Engineering University, in 1982 and 1987, respectively.

His current research interests include wideband signal detection, processing and recognition, and signal processing for communications. He is currently a Senior Member of the China Institute of Communications, a Board Member of the Committee of Deep Space Exploration Technology, Chinese Society of Astronautics, and also a Member of China Society of Image and Graphics.

MINHO JO received the B.A. degree from the Department of Industrial Engineering, Chosun University, South Korea, in 1984, and the Ph.D. degree from the Department of Industrial and Systems Engineering, Lehigh University, USA, in 1994.

He has been one of the founders of the Samsung Electronics LCD Division, since 1994. He is currently the Chairman of the Department of Computer Convergence Software, Korea University, Sejong City, South Korea. He has published over 100 publications in reputed journals/magazines and international conferences. His current research interests include the IoT, blockchain, LTE-Unlicensed, artificial intelligence and big data, network security, HetNets, cloud/fog computing, wireless energy harvesting, autonomous cars, and optimization and probability in networks. He was a recipient of the 2018 IET Best Paper Premium Award. He received the Headong Outstanding Scholar Prize, in 2011. He was the Vice President of the IEIE (Institute of Electronics and Information Engineers) and is currently the Vice President of the KSII (Korean Society for Internet Information). He is the Founder and an Editor-in-Chief of the *KSII Transactions on Internet and Information Systems* (SCI/JCR and SCOPUS indexed) and is the Founder of the *IEIE Transactions on Smart Processing and Computing* (SCOPUS indexed). He is currently an Associate Editor of IEEE Access and an Editor of the IEEE Wireless Communications and the IEEE Internet of Things Journal. He is an Associate Editor of the *MDPI Electronics*, *Security and Communication Networks*, and *Wireless Communications and Mobile Computing*.